HHS Public Access

Author manuscript

Biomaterials. Author manuscript; available in PMC 2019 April 01.

Published in final edited form as:

Biomaterials. 2018 April ; 161: 216–227. doi:10.1016/j.biomaterials.2018.01.040.

Harnessing Macrophage-Mediated Degradation of Gelatin Microspheres for Spatiotemporal Control of BMP2 Release

Ramkumar T. Annamalai[1,*], **Paul A. Turner**[1], **William F. Carson IV**[2], **Benjamin Levi**[3], **Steven Kunkel**[2], and **Jan P. Stegemann**[1,*]

[1]Department of Biomedical Engineering, University of Michigan, Ann Arbor

[2]Department of Pathology, University of Michigan, Ann Arbor

[3]Department of Surgery, University of Michigan, Ann Arbor

Abstract

Biomaterials-based approaches to harnessing the immune and inflammatory responses to potentiate wound healing hold important promise. Bone fracture healing is characterized by an acute inflammatory phase, followed by a transition to a regenerative and repair phase. In this study, we developed genipin-crosslinked gelatin microspheres designed to be preferentially degraded by inflammatory (M1) macrophages. Highly crosslinked (>90%) microspheres allowed efficient incorporation of bioactive bone morphogenetic protein 2 (BMP2), a potent stimulator of osteogenesis in progenitor cells, via electrostatic interactions. Release of BMP2 was directly correlated with degradation of the gelatin matrix. Exposure of microspheres to polarized murine macrophages showed that degradation was significantly higher in the presence of M1 macrophages, relative to alternatively activated (M2) macrophages and unpolarized controls. Microsphere degradation in the presence of non-inflammatory cells resulted in very low degradation rates. The expression of matrix metalloproteinases (MMPs) and tissue inhibitors of MMP (TIMPs) by macrophages were consistent with the observed phenotype-dependent degradation rates. Indirect co-culture of BMP2-loaded microspheres and macrophages with isolated adipose-derived mesenchymal stem cells (MSC) showed that M1 macrophages produced the strongest osteogenic response, comparable to direct supplementation of the culture medium with BMP2. Controlled release systems that are synchronized with the inflammatory response have the potential to provide better spatiotemporal control of growth factor delivery and therefore may improve the outcomes of recalcitrant wounds.

Keywords

Macrophages; inflammation; BMP; immunomodulation; bone tissue engineering; controlled drug release

[*]Corresponding Authors: Jan P. Stegemann, Ramkumar T. Annamalai, Department of Biomedical Engineering, University of Michigan, 1101 Beal Ave., Ann Arbor, MI 48109, Tel: 734-764-8313, Fax: 734-647-4834, jpsteg@umich.edu (JPS), ramta@umich.edu (RTA).

1. Introduction

Inflammation is a key regulator of the regeneration process that helps to determine the course and extent of bone regeneration [1]. Bone defects are extensively infiltrated by immune cells that play an important role in modulating the inflammatory response via secreted factors. In particular, macrophages are key immune cells that actively participate in the evolution of the inflammatory response by shifting from an inflammatory phenotype (M1) to a regenerative phenotype (M2) as healing progresses [2, 3]. The spatial and temporal balance between these two phenotypic states is a key to full functional recovery after injury (reviewed in [4]). Harnessing the inflammatory response via biomaterials-based approaches is a growing field of interest, because of the potential to regulate and accelerate tissue regeneration [5–8].

Bone fracture healing involves both anabolic and catabolic processes that work in tandem to regenerate tissue volume and promote appropriate remodeling over time [9]. These metabolic processes occur in three biological phases: inflammation, endochondral ossification and coupled remodeling (Fig. 1A). The inflammatory phase (peaking at day 1–3) results in the formation of a hematoma and recruitment of both osteoprogenitor and inflammatory cells to the wound site. The recruited inflammatory cells, mainly macrophages, then induce resident osteoprogenitor cells to differentiate, which leads to the formation of a callus during the endochondral phase (day 5–10). The transition from inflammatory to a tissue regeneration phases is assisted by a concomitant shift in local macrophage phenotype from pro-inflammatory toward pro-repair. It has been shown that osteoinductive signals are maximally beneficial when applied during the late inflammatory period that precedes the endochondral phase [9], making this the optimal therapeutic window for delivering osteoinductive factors. Appropriately-timed cytokine delivery, therefore, can lead to enhanced progenitor cell commitment, which leads to increased callus size and stiffness, as well as subsequent remodeling to mature ossified tissue [9].

Each year in the United States, more than half a million patients receive bone defect repairs, out of which over 100,000 cases are due to nonunion fractures that rarely heal without secondary intervention [10, 11]. Non-healing fractures often show an early or even an extended inflammatory phase (Fig. 1B), but are typically characterized by an impaired endochondral phase, due to inadequate blood supply or a poor cellular or cytokine response [1]. Various strategies have been explored for augmenting bone regeneration in recalcitrant fractures and in patients with limited healing capacity. While autografts remain the most common clinical option, they are of limited availability and can cause donor-site morbidity and pain [12–14]. Allogeneic bone grafts are an alternative, but are hampered by issues of compatibility and disease transmission [15–18]. Engineered bone substitutes made from natural and synthetic [19, 20] polymers are being developed, but a key issue is that these materials by themselves are not naturally osteoinductive. During resorption and remodeling, these materials are generally replaced by dense collagenous tissue which does not provide the mechanical stability and functionality of native bone. For these reasons, there is great interest in potentiating the development of new mature bone through the release of osteoinductive factors.

Bone morphogenetic protein 2 (BMP2) is a member of the transforming growth factor beta (TGF-β) super-family of proteins and has been shown to be highly osteoinductive through its effects on progenitor cells [21, 22]. This process unfolds via a characteristic pathway of receptor activation that leads to specific signaling cascades involved in osteogenesis [23]. BMP2 has been shown to induce bone formation in both ectopic and orthotopic sites in animal models [24, 25] as well as in clinical trials [26, 27]. It is particularly essential for the initiation of fracture repair [24] and consequently has been used as a therapeutic agent to accelerate bone regeneration. However, the efficacy of BMP2 therapy is highly dependent on the method of delivery to the target site. Systemic delivery is inefficient and topical administration often results in washout of the protein from the target site [28]. BMP2 delivery from biomaterial scaffolds has been investigated, but rapid hydration or dissolution of the carrier can similarly result in washout [29]. To compensate for this loss, BMP2 is often administered at high concentrations, which increases the risk of bone overgrowth, heterotopic ossification and other complications [30–32]. High doses of BMP2 have also been associated with systemic inflammation and the generation of reactive oxygen species, which can lead to serious consequences.[33, 34]. Therefore, there is a need for methods to both spatially and temporally control the release of BMP2, to maximize its therapeutic effect at doses that are safe.

The strategy in the present study was to create a BMP2 delivery system that is responsive to the inflammatory environment, resulting in efficient and spatiotemporally controlled initiation of the endochondral phase of bone regeneration. We developed crosslinked gelatin microspheres that sequester BMP2 and which are designed to be delivered in a minimally invasive manner to sites of bone injury (Fig. 2A). These microspheres are preferentially degraded by macrophages of the inflammatory phenotype, which enables the release of BMP2 during the optimal therapeutic window for initiating the transition to the endochondral phase during fracture repair (Fig. 2B). The degradation of microspheres and the release kinetics of BMP2 release were characterized using enzymatic treatment and by culturing with inflammatory (M1) and regenerative (M2) macrophages in both two- and three-dimensional culture systems. Also, the mechanism by which M1 macrophages more aggressively degrade microspheres was examined and was compared to M2 macrophages and other non-inflammatory cells commonly implicated in fracture healing. Finally, we show that inflammatory macrophage-mediated release of BMP2 from gelatin microspheres has the effect of promoting osteogenic differentiation in mesenchymal stem cells. Such biomaterial-based approaches can be used to synchronize growth factor release with the inflammatory response, and thereby promote faster and more complete bone regeneration in hard-to-heal defects.

2. Material and Methods

2.1 Cell isolation and culture

Macrophages were derived from monocytes isolated from the bone marrow of C57BL/6 mice as previously described [35]. Briefly, bone marrow was flushed from the long bones, and a single cell suspension was prepared by mechanical disruption and filtering through a 70 μm cell strainer. The cell suspension was then cultured in DMEM supplemented with

15% qualified fetal bovine serum (FBS; Gibco, Saint Aubin, France) and recombinant murine macrophage colony stimulating factor (MCSF, Peprotech, Rocky Hill, NJ) or 30% v/v L-cell supplement for 6 days. The qualified FBS from GIBCO is highly characterized serum containing low endotoxin levels and was chosen for our studies to ensure consistency and to reduce any unintended macrophage activation. The adherent monocyte-derived macrophages were then harvested and used in experiments.

Adipose mesenchymal stromal cells (MSC) were harvested from the inguinal fat pads of C57BL/6 mice as previously described [36, 37]. Briefly, the inguinal fat pads from 6–8 week old mice were harvested and digested using 0.1 wt% collagenase in calcium and magnesium free phosphate buffered saline (PBS; Invitrogen). The obtained single cell suspension was filtered through a 70 μm cell strainer, suspended in Dulbecco's Modified Eagle's Medium (DMEM, Invitrogen) supplemented with 10% qualified FBS and 1% penicillin and streptomycin (Invitrogen) and cultured in tissue culture dishes. Adherent MSC were culture-expanded until passage 6 before use in experiments. Other primary cell lines: human microvascular endothelial cells (EC, Lonza, Allendale, NJ) and human normal lung fibroblasts (FB, Lonza), were obtained from commercial vendors and cultured according to the suppliers' recommendations. Standard osteogenic supplements (OST) were added to the respective expansion media for differentiating MSC.

2.2 Macrophage polarization and characterization

Adherent monocyte-derived macrophages (M0) were maintained in DMEM growth medium supplemented with 10% FBS and 20 ng/mL M-CSF. Macrophages were skewed towards inflammatory (M1) and regenerative (M2) phenotypes by adding suitable supplements to the growth media. For skewing towards M1 phenotype, culture medium was supplemented with 100 ng/mL of IFNγ and 100 ng/mL of lipopolysaccharide (LPS, TLR ligand) and for the M2 phenotype 40 ng/ml of Interleukin-4 (IL4, Peprotech) and 20 ng/ml of IL13 (Peprotech) as previously described [38–40]. Non-activated macrophages (M0) supplied with the maintenance medium were used as controls.

Flow cytometric analysis was performed to characterize phenotypic shifts in macrophages as previously described [5, 38]. Activated (M1, M2) and control (M0) macrophages cultured for at least 36 hours of in the appropriate media were detached using non-enzymatic cell dissociation solution (CellStripper, Sigma) and suspended in ice-cold FACS buffer (Ca^{2+} and Mg^{2+} free PBS, 7% FBS, and 0.1% sodium azide). Cells were centrifuged and blocked with mouse Fc Block solution (R&D Systems, CA) in ice to reduce potential non-specific antibody staining. Diluted (0.1–10 μg/ml) labeled antibody solution was directly added and incubated for at least 30 min at 4°C in the dark. APC anti-mouse CD197 (CCR7) antibody (Biolegend, San Diego, CA) and FITC anti-mouse CD206 (MMR) antibody (Biolegend) were used to identify macrophage phenotypes. Cells were then washed three times in FACS buffer, fixed in 4% formalin, filtered through 80 μm nylon mesh and analyzed in a Coulter CyAn ADP analyzer (Beckman Coulter, Miami, FL). Data were exported as FCS files and analyzed using Summit 4.3 (Beckman Coulter, Inc. Fullerton, CA).

For quantifying cytokine secretion, spent media samples were collected from macrophage cultures at suitable time points and assayed using ELISA kits. Antibodies against TNFα

(R&D Systems), IL-6 (R&D Systems), IL-12 (R&D Systems), IL-10 (R&D Systems), and VEGF (R&D Systems) were quantified to differentiate relative macrophage phenotypes. Macrophages polarized towards the M1 phenotype are characterized by high levels of TNFα, IL-6, IL-12, and VEGF, while M2 macrophages are characterized by high levels of IL-10 secretion in addition to a reduction in M1 cytokines as detailed previously [41]. Gene expression analysis using a 7500 Real-Time PCR System (Applied Biosystems, Foster City, CA) was done to confirm M2 skewing using IL-4 and IL-13 treatment as previously described [42]. TaqMan gene expression assays for mannose receptor (*Mrc1,* Mm00485148_m1), arginase (*Arg1,* Mm00475988_m1), and vascular endothelial growth factor A (*Vegfa,* Mm00437306_m1) were used for the analysis. 18S (*Rn18s*, Mm03928990_g1) was used for loading control. All TaqMan expression reagents were purchased from Applied Biosystems.

2.3 Microspheres preparation and genipin crosslinking

Gelatin microspheres (Gelatin type A, anionic) were made by emulsification of gelatin solution and subsequent cross-linking using genipin. Briefly, gelatin A from porcine skin (175 bloom, Sigma) was dissolved in a stock solution of 6 wt% and added dropwise to a stirred polydimethylsiloxane (PDMS, Clearco Products, Willow Grove, PA) bath at 40°C. The mixture was stirred by a dual radial-blade impeller at 2300 rpm for 5 minutes to disperse the gelatin into a fine emulsion in the PDMS. The emulsion was then cooled to 4°C in an ice bath and stirred for an additional 30 minutes to promote gelation of the microspheres droplets. To separate the microspheres from the emulsion, PBS containing 0.01% v/v Pluronic L101 surfactant (BASF, Florham Park, NJ) was added, vigorously mixed, and centrifuged at 200 g for 5 min. The PDMS supernatant was removed without disturbing the pellet, which was then rewashed with surfactant solution.

Gelatin microspheres were crosslinked using amine-reactive genipin (Wako Chemicals) by suspending the washed microspheres in 1.0 wt% genipin in PBS solution. The degree of cross-linking is dependent on the time of incubation [43], and 12 h crosslinking was used to saturate available amine groups completely. At the end of the reaction, excess solution was removed, and microspheres were washed in ethanol, followed by deionized water to remove reactants. Microspheres were then frozen at −80°C and freeze-dried to remove all residual water. Though gelatin itself shows faint auto-fluorescence, genipin crosslinking imparts a distinct fluorescence response at the 590/620 Ex/Em wavelengths. This distinct fluorescence profile was used to visualize sphere morphology and measure degraded microsphere mass. A standard curve relating known microsphere mass and fluorescence of microspheres after complete solubilization in collagenase was created to measure the degradation rate (See Supplementary Figure S1). The zeta potential of gelatin microspheres in PBS was measured using a Zetasizer (Malvern, Westborough, MA). Zeta potential measurements were performed in Gibco PBS (pH 7.4) to reflect physiological conditions. Since growth factor loading was also performed in PBS, the measured zeta potential is reflective of the charge affinity we anticipate to drive the polyionic complexation. The morphology, sphericity, and size distribution of the microspheres were analyzed from confocal stacks (Nikon A1 Confocal Microscope). ImageJ software (National Institutes of Health) was used to determine the size distribution and sphericity of the microspheres. Imaris software (Bitplane,

Belfast, UK) was used for generating a 3D projection of the confocal stacks. Sphericity is a dimensionless measure of how closely the shape of a microsphere approaches that of a mathematically perfect sphere, and is calculated by ImageJ using area and perimeter measurements of the microspheres. Any particle which is not a perfect sphere will have sphericity less than 1.

Cytotoxicity of the cross-linked microspheres and their degradation products was analyzed by comparing the metabolic activity of different macrophage phenotypes to that of the macrophages cultured along with unloaded gelatin microspheres using PrestoBlue® reagent (Invitrogen). For the metabolic activity assay, 100 μL of Prestoblue® stock solution was added to each culture condition containing 1 ml of phenol-red free DMEM and incubated at 37°C for 30 min. After the incubation period, the solution was transferred to a 96 well plate, and fluorescence readings (excitation/emission 560/610) were taken using a microplate reader.

2.4 Microsphere loading, degradation, and release

Lyophilized microspheres were swelled in PBS and loaded with recombinant mouse/rat/human BMP2 (R&D Systems, Catalog # 355-BM/CF) by incubation in concentrated BMP2 stock solution (80 μg/mL of PBS). For one mg of dry microspheres, 10 μl of the stock solution was supplied. Loading was performed under static conditions overnight at 37 °C. Loaded spheres were subsequently washed in PBS containing 10 mg/mL albumin to remove unbound growth factor. Loading efficacy was determined by comparing BMP2 concentration in solutions taken from the wash buffer of loaded microspheres versus control BMP2 solutions containing no microspheres using BMP2 sandwich ELISA kit (Quantikine BMP-2 ELISA kit, R&D Systems, Catalog # DBP200).

For measurement of enzymatic degradation and release, crosslinked gelatin microspheres were deflocculated by sonification and immersed in purified collagenase (Worthington, CLSPA: Activity ≥ 500 units per mg dry weight) solution. A range of collagenase concentrations (0, 1.0, 5.0, 7.5 and 10 U/mL in M0 macrophage growth media) were tested initially with unloaded microspheres in 24-well plates and kept at 37°C until the microspheres were fully degraded. The solubilized degradation products in the supernatant were quantified fluorometrically (590/620 Ex/Em) every 5 min for 48 hours using a plate reader. To measure BMP2 release, the microspheres loaded with BMP2 were suspended in 5 U/mL of collagenase in M0 macrophage growth media and 200 μL of the supernatant was collected every 24 hours for analysis. Solubilized BMP2 and the degradation products were quantified from the same sample through ELISA and fluorometric analysis respectively. Values were normalized against controls, and the degradation rate was determined based on standards of known concentration. A BMP2 sandwich ELISA kit (Quantikine BMP-2 ELISA kit, R&D Systems) was used to determine the rate of BMP2 release from the degrading microspheres. The samples were diluted appropriately with PBS to be within the working range of the ELISA kit.

For the measurement of macrophage-mediated degradation and release in 2D culture, macrophages were seeded in 24-well non-tissue culture dishes at a density of 5×10^4 cells/cm^2 in control growth medium. After two days, macrophages were shifted to the M1

and M2 phenotype by supplying appropriate supplements. After two more days of macrophage skewing, gelatin microspheres loaded with or without BMP2 were added to the macrophage monolayer at a density of 250 μg/cm^2. Medium was changed partially (15% at each change) every 48 hours without disturbing the settled microspheres. The spent media was analyzed to quantify the degraded gelatin mass and the released BMP2. To account for BMP2 loss during the medium changes, 15% of the measured BMP2 concentration in the previous time points were added to the consecutive time point measurements. For all BMP2 release studies, microspheres without BMP2 served as controls. For 3D analysis, macrophages and microspheres were mixed in 0.5 ml of 2.0 mg/mL of neutralized collagen solution and immediately gelled in 24-well dishes at 37 °C. The concentration of the microspheres and density of macrophages were kept consistent with the 2D cultures.

2.5 Co-culture studies

For co-culture studies with MSC, Transwell™ permeable supports (Corning) with 0.4 μm pore size were used. Macrophages and microspheres were seeded in the Transwell™ insert at a density of 5×10^4 cells/insert and 500 μg/insert respectively. MSC were seeded in the bottom tissue culture-treated dish at 5×10^4 cells/cm^2. The permeable membrane on the Transwell™ insert allowed the paracrine exchange of solutes and growth factors between the compartments. Release of BMP2 from the loaded microspheres was quantified using ELISA, and the effect on the underlying MSC was assessed through analysis of osteogenic gene expression and calcium deposition. For all BMP2 release studies, microspheres suspended in PBS-albumin buffer served as control.

For mineralization studies, MSC were cultured in tissue culture dishes and presented with microspheres and macrophages in permeable Transwell™ inserts. Mineral staining solution (1.0 wt% alizarin red) was prepared by dissolving 1.0 g of alizarin red powder (Sigma) in 100 mL of ultrapure water and adjusting the pH to 4.2. MSC samples were collected after 10 days of co-culturing, rinsed in PBS, fixed in 10% buffered zinc-formalin (Z-Fix, Anatech Ltd), and then washed three times in PBS and twice in deionized water. The wells containing the cell monolayer were then stained with Alizarin-red solution for 10 min. Cells were then washed twice with deionized water and imaged using bright-field microscopy. For quantification of mineral levels, wells were destained in 1.0 mL of 0.5 N HCl/5% sodium dodecyl sulfate solution for 20 min. The destained extracted solution was then quantified colorimetrically by measuring absorbance at 415 nm.

Quantitative polymerase chain reaction (Q-PCR) was used to examine gene expression. MSC were harvested after 10 days of co-culture, and total RNA was isolated using TRIzol reagent (Invitrogen, Carlsbad, CA) according to the manufacturer's instruction. Our standard protocol is to collect samples at day 0, 7, 14 and 21 for most assays. However, we chose the day 10 time point for the macrophage co-cultures because it provided sufficient time for the degradation of microspheres and concomitant release of BMP2 to have a detectable influence over the phenotype of the MSC. This time point also avoided interference from inflammatory cytokines released by macrophages in longer-term cultures (>14 days), which can also affect MSC phenotype. Total RNA was quantified using a spectrophotometer (NanoDrop Technologies, Wilmington, DE). Reverse transcription was performed at 38 °C

for 60 min to yield cDNA and the reaction was stopped by incubation at 94 °C for 10 min. Gene expression was analyzed using a 7500 Real-Time PCR System (Applied Biosystems, Foster City, CA). TaqMan gene expression assays for osteocalcin (*Bglap,* Mm03413826_mH), osteopontin (*Spp1,* Mm00436767_m1), alkaline phosphatase (*Alp1*, Mm00475834_m1), and BMP2 (*Bmp2,* Mm01340178_m1) were used to analyze MSC phenotypes in co-culture experiments. TaqMan gene expression assays for TIMP1 (*Timp1,* Mm01341361_m1), TIMP2 (*Timp2,* Mm00441825_m1), MMP2 (*Mmp2,* Mm00439498_m1), and MMP9 (*Mmp9,* Mm00442991_m1) were used to analyze macrophage phenotypes. GAPDH (*Gapdh*, 43083130) was used for loading control. All TaqMan expression reagents were purchased from Applied Biosystems.

Quantification of total DNA was performed using a commercially available double-stranded DNA assay kit (Quanti-iT PicoGreen, Invitrogen, Life Technologies) as described previously [44, 45]. Collagen gels containing cells were washed in PBS, homogenized by sonication at 30% intensity for 3 sec in ice and digested in 50 mmol/L Tris-HCl/4 mol Guanidine-HCl solution (pH 7.5) for 2–3 hours at 4 °C. Digested samples were then centrifuged at 5000 g, and the samples were diluted five times in deionized water to reduce the guanidine concentration to <150 mmol/L to avoid interference. The DNA content of the supernatant was then quantified using 1x PicoGreen in Tris-HCl buffer added to the diluted samples by measuring fluorescence at EX:485, EM:518 nm after 5 min incubation. Purified calf thymus DNA served as the standard for the assay.

2.6 Statistical Analysis

All measurements were performed at least in triplicate. Data are presented as mean ± one standard deviation. Statistical analysis was done using Student's *t*-test with a 95% confidence limit, and two-way ANOVA was used for multi-group comparisons. Differences were considered statistically significant at a level of $p<0.05$.

3. Results

3.1. Characterization of BMP2-loaded gelatin microspheres

The oil-in-water emulsification of solubilized gelatin yielded microspheres with the sphericity of 0.88±0.1 (Fig. 3A) and an average diameter of 12.4±2.9 μm (Fig. 3B). The degree of crosslinking of these microspheres can be controlled via the time of exposure to genipin [43]. Furthermore, the degradability of the microspheres depends on the degree of crosslinking, which allows tailoring of the degradability. In this study, microspheres were treated to ensure crosslinking of >90% of the available primary amines in the gelatin structure. Crosslinking with genipin (Fig. 3C) occurs through a two-step process where the primary amines of gelatin polypeptides form stable intermediates through Michael addition, followed by nucleophilic substitution with the ester group in genipin to form a secondary amide link. This reaction imparted a net negative charge on the crosslinked microspheres. The zeta potential (ζ) in PBS was found to be −5 mV, thereby imparting an affinity for positively charged proteins at physiological conditions such as BMP2 (pI of 8.5–9.5).

Degradation of microspheres using different concentrations of collagenase at 37°C (Fig. 3D) demonstrated a dose-dependence. Under both control conditions (M0 culture medium) and low collagenase concentration (1.0 g/mL), degradation was negligible over 48 hours. At high collagen concentrations (7.5 and 10 mg/mL), there was very rapid initial degradation, followed by a plateau. At a concentration of 5.0 mg/mL collagenase, microsphere degradation was steady and sustained over 48 hours, and this concentration was therefore used to subsequently characterize BMP2 release from microspheres. BMP2 was loaded into the crosslinked microspheres through electrostatic sequestration of the positively charged growth factor by the negatively charged and crosslinked gelatin matrix. More than 75% of the supplied BMP2 was loaded into the microspheres in the first 24 hours, and the total loading capacity of the microspheres was calculated to be 640 ng of BMP2 per mg of microspheres. In degradation experiments, microspheres exhibited an initial burst release, followed by linear and sustained release of approximately ~440 ng of BMP2 over a period of 24 hours. BMP2 release and microsphere degradation rate were highly correlated ($R=0.95$, $p<0.05$, Fig. 3E, see supplementary Figure S2 for BMP2 release over time).

3.2. Macrophage phenotype and cell-mediated degradation of microspheres

The shift in macrophage phenotypes in the presence of relevant polarizing stimuli was characterized using flow cytometry (for 2D cultures) and cytokine secretion assay (for 3D collagen gels). Flow cytometric analysis (Fig. 4A), showed that within 24 hours of culture in the presence of M1 stimuli (IFNγ and LPS), macrophages exhibited increased CD197 (CCR7) expression and reduced CD206 (MMR, mannose receptor) expression. Similarly, macrophages cultured in the presence of M2 stimuli (IL-4, IL-13), showed increased CD206 expression and reduced CD197 expression. The morphology of the cells (Fig. 4B) also changed to reflect the respective phenotypes, with M1 macrophages showing a ‘broken-egg’ morphology while the M2 macrophages are exhibiting more spindle-shaped morphology. Analysis of the cytokine release profile (Fig. 4C) similarly confirmed the observed phenotype shift. M1 macrophages secreted significantly higher levels of TNFα, IL-6, while M2 macrophages had markedly reduced secretion relative to M1. Both M1 and M2 macrophages exhibited increased secretion of IL-10, relative to unpolarized controls. Upregulation of mannose receptor C type-I (*Mrc1*) and arginase (*Arg1*) gene expression levels and downregulation of vascular endothelial growth factor (*Vegfa*) gene expression, further confirmed M2 skewing using IL-4 and IL-13 treatment (See supplementary Figure S3).

Macrophage-mediated biodegradation of the gelatin microspheres and release of BMP2 was investigated in the presence of M1 and M2 stimuli, in both 2D culture as well as in 3D collagen matrices. Images of macrophages cultured with gelatin microspheres (Fig. 5A, insets show fluorescent gelatin microspheres) showed a close association between the cells and the microspheres, and that the microspheres degraded over time. The genipin crosslinking changed the color of the gelatin microspheres to a blue/purple color under visible light. The degradation rate varied between macrophage phenotypes and culture formats. At the same cell density and microsphere mass, the rate of degradation of microspheres was higher in 2D culture wells, compared to that in 3D collagen matrices (Fig. 5B). In both culture formats, M1 macrophages degraded the microspheres significantly more

rapidly than M2 or M0 (unpolarized control) cells. The DNA normalized degradation rate at day 10 (inset Fig 5B) further confirmed that the microsphere degradability is phenotype specific and not merely due to variability in cell density. The release of BMP2 from loaded microspheres in 3D cultures (Fig. 5C) followed a similar trend, with significantly higher BMP2 release stimulated by M1 macrophages relative to M0 and M2 cells.

A high degree of crosslinking (>90%) of the gelatin microspheres was specifically used in this study to preferentially promote degradation by inflammatory macrophages. Degradation of microspheres by non-inflammatory cells often found in the wound healing milieu was also characterized, including murine adipose-derived mesenchymal stromal cells (MSC), osteogenically differentiating MSC (O-MSC), human microvascular endothelial cells (EC), and human fibroblasts (FB). In 2D culture wells (Fig. 6A), the rate at which microspheres were degraded was very low for all non-inflammatory cell types, relative to M1 macrophages. In 3D collagen matrix culture (Fig. 6B), the degradation rate by MSC, O-MSC, and EC was higher than in 2D, but still markedly lower than for M1 macrophages.

To better understand how macrophage phenotype is related to gelatin microsphere degradation, the levels of key proteolytic enzymes and their inhibitors were examined. MMP2 and MMP9 are the main gelatinases involved in tissue remodeling, and TIMP2 and TIMP1 are respective primary inhibitors of these enzymes [46]. Expression of MMP2 was significantly higher in M1 macrophages compared to M2 macrophages (Fig. 7A), while MMP9 was significantly decreased relative to unpolarized cells. Conversely, TIMP1 expression (Fig. 7B) was substantially increased in M2 macrophages, and suppressed in M1 cells, relative to the M0 control. TIMP2 expression was also essentially abrogated in M1 macrophages, but not statistically changed in M2 cells.

3.3. Macrophage-mediated release of BMP2 and osteogenic differentiation of MSC

The functional efficacy of BMP2-loaded microspheres and in response to their degradation by polarized macrophages was tested by co-culturing microspheres and macrophages in a 3D collagen gel in a Transwell™ insert, with a monolayer of MSC cultured in the corresponding underlying culture well (Fig. 8A). This allowed macrophages to be stimulated to shift phenotypes, and thereby exert paracrine effects on the co-cultured MSC. Cultures prepared with macrophages and unloaded microspheres were used as controls. After 10 days in culture, co-cultures using M1 macrophages resulted in upregulation of the key osteogenic markers alkaline phosphatase (ALP), osteopontin, and BMP2, relative to cultures with unloaded microspheres (Fig. 8B, $p<0.05$). Note that the data in Fig. 8B are also normalized to the quantity of macrophages in each treatment since the macrophages caused microsphere degradation, but their proliferation was phenotype-dependent. Non-normalized data are shown in supplementary Figure S4. M2 macrophage-mediated cultures increased expression of osteocalcin and osteopontin, but inhibited the other markers. The increase in the expression of osteogenic genes was similar to the response seen in the positive control (Fig. 8C, 8D), in which MSC were exposed to a constant dose of 200 ng/ml of solubilized BMP2 delivered directly in the culture medium.

The same co-culture system was used to investigate mineral deposition by MSC in response to macrophage-mediated BMP2 release from microspheres. Direct supplementation of the

culture medium with 200 ng/mL of BMP2 was again used as a positive control while unloaded microspheres served as negative controls. At day 10, both phase contrast imaging and calcium staining (Fig. 9) showed that M1 macrophages elicited the highest mineralization response, similar to the positive control. Microsphere co-cultures with M0 and M2 macrophages produced very little matrix mineralization, consistent with the corresponding gene expression seen in M0, M1 and M2 conditions. The negative controls with unloaded microspheres (insets Fig. 9) did not show any detectable mineralization in any macrophage phenotype condition.

4. Discussion

There is growing recognition that harnessing inflammatory and immune responses can be a powerful tool in promoting tissue regeneration and curing disease [5–8]. The field of biomaterials has embraced this approach through the design and application of materials that direct and/or enhance physiological responses. While the inflammatory response is complex, an important aspect in developing translatable therapies is to target key processes that can be modulated with a relatively simple strategy. The harnessing of inflammatory macrophages to enable spatial and temporal control of defined growth factor release is one such strategy that could improve healing outcomes.

The conventional view of macrophages as primarily immune-activating cells is being reevaluated, as additional phenotypes of macrophages have been identified with a range of functions [2, 3, 47]. Macrophages retain remarkable plasticity, and their phenotype is influenced by their environment. In general, pro-inflammatory M1 macrophages dominate the injury site during the early stages of healing, while pro-regenerative M2 macrophages become more prevalent during the later remodeling stages. Our approach in this study was to create gelatin microspheres as growth factor delivery vehicles that are particularly relevant in the early inflammatory stage of bone healing, as a tool to promote the transition to the following endochondral ossification stage of healing. These microspheres were designed to tightly sequester the potent osteogenic growth factor BMP2, and to be preferentially degradable only by activated M1 macrophages.

Gelatin is derived from the controlled hydrolysis of collagen, and therefore has a similar amino acid structure and can form a gel at relatively low concentrations [48]. An advantage of gelatin polypeptides is that the net charge can be varied by controlling the conditions of hydrolysis [49], and they are generally less immunogenic than full-length collagen due to the removal of aromatic groups [50, 51]. We employed a simple water-in-oil emulsification method [43, 52] to produce gelatin microspheres on the same size scale as cells (10–20 μm). Since gelatin has a sol-gel transition near 30° C, it is necessary to crosslink the matrix to produce microspheres that are stable at physiological temperatures. The method and extent of crosslinking determine the swelling ratio, mechanical properties, and resistance to enzymatic degradation of peptide materials [53, 54], and can also influence the antigenicity. A variety of chemical agents, including formaldehyde [55], glyceraldehyde [56] and glutaraldehyde [57], have been used to crosslink gelatin, however, there is concern about their toxicity [58]. We, therefore, chose genipin as a crosslinking agent, because it has been shown to be significantly less toxic than other compounds [58]. Genipin also has the

advantage that the degree of crosslinking can be controlled through the concentration and incubation time [43, 59], and it results in a matrix with a net negative charge, which is useful to sequester positively charged molecules. This allowed BMP2 (pI = 8.5 [60]) to be loaded into gelatin microspheres via polyionic complexation [61]. We have shown that growth factors are efficiently and very tightly bound via this method, and are only released via degradation of the microspheres over time [43, 52].

Our results show that highly crosslinked gelatin microspheres release biologically active BMP2 upon active degradation either by purified collagenase or via enzymes secreted by inflammatory macrophages. Importantly, other non-inflammatory cells that are also involved in tissue repair do not effectively degrade these microspheres. This differential ability to release BMP2 from gelatin microspheres confers an ability to target the effects of this potent cytokine to areas and timeframes in which M1 macrophages are particularly active. Macrophages secrete a variety of matrix metalloproteinases (MMPs) that function to degrade the extracellular matrix [62], and the panel of MMPs produced is known to vary with macrophage phenotype [63]. MMP2 and MMP9 are the major gelatinases. Our experiments showed that the ratio of MMP to TIMP expression was elevated particularly in M1 macrophages, relative to the M2 phenotype. These findings are consistent with other studies that have shown that MMP2 and MMP9 are increased in response to inflammatory signals [64, 65], while their secretion is negatively influenced by the M2 phenotype-promoting cytokines [66, 67]. Matrix degradation is also regulated by tissue inhibitors of MMPs (TIMPS). Our experiments showed very strong downregulation of TIMP1 and TIMP2, two of the major inhibitors of MMP activity, in M1 macrophages. In contrast, TIMP expression in the pro-repair M2 macrophage phenotype was elevated relative to M1, suggesting a protective effect on new matrix being produced. We also observed higher gelatin degradation rates in 2D cultures compared to 3D hydrogels, possibly due to enhanced MMP secretion by macrophages, which has been observed in 2D culture [63]. The balance between MMP and TIMP expression regulates tissue degradation and regeneration, and therefore can also be used to modulate degradation-mediated release from gelatin microspheres.

The ability of BMP2-loaded gelatin microspheres to promote osteogenesis in progenitor cells was also evaluated as a functional test. Delivery of BMP2 via degradation of gelatin microspheres by M1 macrophages clearly potentiated the expression of osteogenic markers, particularly the early marker alkaline phosphatase (ALP) and the late marker osteopontin (OPN). Although not always evident under in vitro conditions, it should be noted that inflammatory macrophages may themselves induce osteogenesis over prolonged exposure periods (>14 days) [68]. Expression of the non-collagenous bone proteins osteocalcin and osteopontin was elevated in cultures with M2 macrophages, suggesting they may have additional effects beyond the release of BMP2. The impact on MSC of BMP2 release from gelatin microspheres was similar to the response to culture medium directly supplemented with 200 ng/mL of soluble BMP2, however, in implantation situations, this unbound growth factor would be very rapidly washed out and therefore its therapeutic effect would be reduced. These studies also validated that the degradation products of the microspheres neither interfere with the bioactivity of BMP2 nor produce any adverse effects on cell function (for cytotoxicity analysis refer supplementary Figure S5).

5. Conclusion

Genipin-crosslinked gelatin microspheres can be produced using a facile water-in-oil emulsification method, and appropriate post-processing allows tailoring of the degree of crosslinking and the charge on the gelatin matrix. Negatively charged microspheres can be efficiently loaded with BMP2, which is released upon degradation by cells. A high degree of crosslinking results in targeted degradation by inflammatory macrophages, since other non-inflammatory cell types, degrade the matrix at much lower rates. The enhanced degradation capacity exhibited by M1 macrophages is a result of coordinated expression of MMPs and TIMPs. The BMP2 that is released from microspheres is active and can induce osteogenesis in local progenitor cells via paracrine signaling. These studies demonstrate that macrophage-mediated degradation of gelatin microspheres can be used to control the spatial and temporal release profile of growth factors. Importantly, the release is triggered during the inflammatory phase of bone healing, such that cytokines are delivered in the optimal therapeutic window to promote bone regeneration. Such inflammation-mediated release systems may find general utility in enhancing wound healing and particularly in preventing fracture non-unions.

Supplementary Material

Refer to Web version on PubMed Central for supplementary material.

Acknowledgments

We acknowledge Melissa Scola of Dr. Kunkel's lab for her assistance with the MMP and TIMP gene expression analysis. Research reported in this publication was supported in part by the National Institute of Arthritis and Musculoskeletal and Skin Diseases (R01AR062636, to JPS), the National Institute of Dental and Craniofacial Research (R01DE026630, to JPS), and the National Science Foundation (DMR 1641065, to JPS and PAT). BL is supported by funding from NIH/National Institute of General Medical Sciences Grant K08GM109105-0, NIH/National Institute of Health R01 GM123069 and R01 AR071379, American College of Surgeons Clowes Award and the International FOP Association. The content is solely the responsibility of the authors and does not necessarily represent the official views of the National Institutes of Health.

References

1. Claes L, Recknagel S, Ignatius A. Fracture healing under healthy and inflammatory conditions. Nature reviews Rheumatology. 2012; 8(3):133–143. [PubMed: 22293759]
2. Spiller KL, Freytes DO, Vunjak-Novakovic G. Macrophages modulate engineered human tissues for enhanced vascularization and healing. Annals of biomedical engineering. 2015; 43(3):616–27. [PubMed: 25331098]
3. Mountziaris PM, Mikos AG. Modulation of the Inflammatory Response for Enhanced Bone Tissue Regeneration, Tissue engineering. Part B. Reviews. 2008; 14(2):179–186.
4. Brown BN, Ratner BD, Goodman SB, Amar S, Badylak SF. Macrophage polarization: An opportunity for improved outcomes in biomaterials and regenerative medicine. Biomaterials. 2012; 33(15):3792–3802. [PubMed: 22386919]
5. Spiller KL, Nassiri S, Witherel CE, Anfang RR, Ng J, Nakazawa KR, Yu T, Vunjak-Novakovic G. Sequential delivery of immunomodulatory cytokines to facilitate the M1-to-M2 transition of macrophages and enhance vascularization of bone scaffolds. Biomaterials. 2015; 37:194–207. [PubMed: 25453950]
6. Kim YH, Furuya H, Tabata Y. Enhancement of bone regeneration by dual release of a macrophage recruitment agent and platelet-rich plasma from gelatin hydrogels. Biomaterials. 2014; 35(1):214–24. [PubMed: 24125774]

7. Hao S, Meng J, Zhang Y, Liu J, Nie X, Wu F, Yang Y, Wang C, Gu N, Xu H. Macrophage phenotypic mechanomodulation of enhancing bone regeneration by superparamagnetic scaffold upon magnetization. Biomaterials. 2017; 140:16–25. [PubMed: 28623721]
8. Gower RM, Boehler RM, Azarin SM, Ricci CF, Leonard JN, Shea LD. Modulation of leukocyte infiltration and phenotype in microporous tissue engineering scaffolds via vector induced IL-10 expression. Biomaterials. 2014; 35(6):2024–31. [PubMed: 24309498]
9. Einhorn TA, Gerstenfeld LC. Fracture healing: mechanisms and interventions. Nature reviews Rheumatology. 2015; 11(1):45–54. [PubMed: 25266456]
10. Amini AR, Laurencin CT, Nukavarapu SP. Bone Tissue Engineering: Recent Advances and Challenges. 2012; 40(5):363–408.
11. Hak DJ, Fitzpatrick D, Bishop JA, Marsh JL, Tilp S, Schnettler R, Simpson H, Alt V. Delayed union and nonunions: Epidemiology, clinical issues, and financial aspects. Injury. 2014; 45(Supplement 2):S3–S7.
12. Silber JS, Anderson DG, Daffner SD, Brislin BT, Leland JM, Hilibrand AS, Vaccaro AR, Albert TJ. Donor Site Morbidity After Anterior Iliac Crest Bone Harvest for Single-Level Anterior Cervical Discectomy and Fusion. Spine. 2003; 28(2):134–139. [PubMed: 12544929]
13. Giannoudis PV, Dinopoulos H, Tsiridis E. Bone substitutes: An update. Injury. 2005; 36(3, Supplement):S20–S27. [PubMed: 16188545]
14. Dimitriou R, Mataliotakis GI, Angoules AG, Kanakaris NK, Giannoudis PV. Complications following autologous bone graft harvesting from the iliac crest and using the RIA: A systematic review. Injury. 2011; 42(Supplement 2):S3–S15.
15. Moreau MF, Gallois Y, Baslé MF, Chappard D. Gamma irradiation of human bone allografts alters medullary lipids and releases toxic compounds for osteoblast-like cells. Biomaterials. 2000; 21(4): 369–376. [PubMed: 10656318]
16. Lewandrowski K-U, Rebmann V, Päßler M, Schollmeier G, Ekkernkamp A, Grosse-Wilde H, Tomford WW. Immune response to perforated and partially demineralized bone allografts. J Orthop Sci. 2001; 6(6):545–555. [PubMed: 11793178]
17. Tomford WW. Transmission of Disease through Transplantation of Musculoskeletal Allografts. Journal of Bone and Joint Surgery-American Volume. 1995; 77a(11):1742–1754.
18. Mroz TE, Joyce MJ, Steinmetz MP, Lieberman IH, Wang JC. Musculoskeletal allograft risks and recalls in the United States. The Journal of the American Academy of Orthopaedic Surgeons. 2008; 16(10):559–65. [PubMed: 18832599]
19. Nandi SK, Roy S, Mukherjee P, Kundu B, De DK, Basu D. Orthopaedic applications of bone graft & graft substitutes: a review. Indian J Med Res. 2010; 132:15–30. [PubMed: 20693585]
20. Henkel J, Woodruff MA, Epari DR, Steck R, Glatt V, Dickinson IC, Choong PF, Schuetz MA, Hutmacher DW. Bone Regeneration Based on Tissue Engineering Conceptions - A 21st Century Perspective. Bone Res. 2013; 1(3):216–48. [PubMed: 26273505]
21. Chen D, Zhao M, Mundy GR. Bone Morphogenetic Proteins. Growth Factors. 2004; 22(4):233–241. [PubMed: 15621726]
22. Blobe GC, Schiemann WP, Lodish HF. Role of Transforming Growth Factor β in Human Disease. New England Journal of Medicine. 2000; 342(18):1350–1358. [PubMed: 10793168]
23. Salazar VS, Gamer LW, Rosen V. BMP signalling in skeletal development, disease and repair. Nat Rev Endocrinol. 2016; 12(4):203–21. [PubMed: 26893264]
24. Tsuji K, Bandyopadhyay A, Harfe BD, Cox K, Kakar S, Gerstenfeld L, Einhorn T, Tabin CJ, Rosen V. BMP2 activity, although dispensable for bone formation, is required for the initiation of fracture healing. Nat Genet. 2006; 38(12):1424–1429. [PubMed: 17099713]
25. Wu G, Liu Y, Iizuka T, Hunziker EB. The effect of a slow mode of BMP-2 delivery on the inflammatory response provoked by bone-defect-filling polymeric scaffolds. Biomaterials. 2010; 31(29):7485–7493. [PubMed: 20638718]
26. Govender S, Csimma C, Genant HK, Valentin-Opran A, Amit Y, Arbel R, Aro H, Atar D, Bishay M, Borner MG, Chiron P, Choong P, Cinats J, Courtenay B, Feibel R, Geulette B, Gravel C, Haas N, Raschke M, Hammacher E, van der Velde D, Hardy P, Holt M, Josten C, Ketterl RL, Lindeque B, Lob G, Mathevon H, McCoy G, Marsh D, Miller R, Munting E, Oevre S, Nordsletten L, Patel A, Pohl A, Rennie W, Reynders P, Rommens PM, Rondia J, Rossouw WC, Daneel PJ, Ruff S,

Ruter A, Santavirta S, Schildhauer TA, Gekle C, Schnettler R, Segal D, Seiler H, Snowdowne RB, Stapert J, Taglang G, Verdonk R, Vogels L, Weckbach A, Wentzensen A, Wisniewski T. B.M.P.E.i.S.f.T.T.S. Group. Recombinant human bone morphogenetic protein-2 for treatment of open tibial fractures: a prospective, controlled, randomized study of four hundred and fifty patients. The Journal of bone and joint surgery American volume. 2002; 84-A(12):2123–34. [PubMed: 12473698]

27. McKay WF, Peckham SM, Badura JM. A comprehensive clinical review of recombinant human bone morphogenetic protein-2 (INFUSE® Bone Graft). International Orthopaedics. 2007; 31(6): 729–734. [PubMed: 17639384]
28. Poynton AR, Lane JM. Safety profile for the clinical use of bone morphogenetic proteins in the spine. Spine. 2002; 27(16):S40–S48. [PubMed: 12205419]
29. Jansen JA, Vehof JWM, Ruhé PQ, Kroeze-Deutman H, Kuboki Y, Takita H, Hedberg EL, Mikos AG. Growth factor-loaded scaffolds for bone engineering. Journal of Controlled Release. 2005; 101(1–3):127–136. [PubMed: 15588899]
30. Garrison KR, Shemilt I, Donell S, Ryder JJ, Mugford M, Harvey I, Song F, Alt V. Bone morphogenetic protein (BMP) for fracture healing in adults. Cochrane Db Syst Rev. 2010; (6)
31. Carragee EJ, Hurwitz EL, Weiner BK. A critical review of recombinant human bone morphogenetic protein-2 trials in spinal surgery: emerging safety concerns and lessons learned. Spine Journal. 2011; 11(6):471–491. [PubMed: 21729796]
32. Shields LB, Raque GH, Glassman SD, Campbell M, Vitaz T, Harpring J, Shields CB. Adverse effects associated with high-dose recombinant human bone morphogenetic protein-2 use in anterior cervical spine fusion. Spine (Phila Pa 1976). 2006; 31(5):542–7. [PubMed: 16508549]
33. Zara JN, Siu RK, Zhang X, Shen J, Ngo R, Lee M, Li W, Chiang M, Chung J, Kwak J, Wu BM, Ting K, Soo C. High Doses of Bone Morphogenetic Protein 2 Induce Structurally Abnormal Bone and Inflammation In Vivo. Tissue Engineering Part A. 2011; 17(9–10):1389–1399. [PubMed: 21247344]
34. Shields LBE, Raque GH, Glassman SD, Campbell M, Vitaz T, Harpring J, Shields CB. Adverse effects associated with high-dose recombinant human bone morphogenetic protein-2 use in anterior cervical spine fusion. Spine. 2006; 31(5):542–547. [PubMed: 16508549]
35. Weischenfeldt J, Porse B. Bone Marrow-Derived Macrophages (BMM): Isolation and Applications. Cold Spring Harbor Protocols. 2008; 2008(12) pdb.prot5080.
36. Gimble JM, Bunnell BA, Frazier T, Rowan B, Shah F, Thomas-Porch C, Wu X. Adipose-derived stromal/stem cells: A primer. Organogenesis. 2013; 9(1):3–10. [PubMed: 23538753]
37. Gimble JM, Katz AJ, Bunnell BA. Adipose-Derived Stem Cells for Regenerative Medicine. Circulation Research. 2007; 100(9):1249–1260. [PubMed: 17495232]
38. Kittan NA, Allen RM, Dhaliwal A, Cavassani KA, Schaller M, Gallagher KA, Carson WFIV, Mukherjee S, Grembecka J, Cierpicki T, Jarai G, Westwick J, Kunkel SL, Hogaboam CM. Cytokine Induced Phenotypic and Epigenetic Signatures Are Key to Establishing Specific Macrophage Phenotypes. PloS one. 2013; 8(10):e78045. [PubMed: 24205083]
39. Hsieh JY, Smith TD, Meli VS, Tran TN, Botvinick EL, Liu WF. Differential regulation of macrophage inflammatory activation by fibrin and fibrinogen. Acta Biomaterialia. 2017; 47(Supplement C):14–24. [PubMed: 27662809]
40. Spiller KL, Wrona EA, Romero-Torres S, Pallotta I, Graney PL, Witherel CE, Panicker LM, Feldman RA, Urbanska AM, Santambrogio L, Vunjak-Novakovic G, Freytes DO. Differential gene expression in human, murine, and cell line-derived macrophages upon polarization. Experimental cell research. 2016; 347(1):1–13. [PubMed: 26500109]
41. Martinez FO, Gordon S. The M1 and M2 paradigm of macrophage activation: time for reassessment. F1000Prime Rep. 2014; 6:13. [PubMed: 24669294]
42. Ishii M, Wen H, Corsa CA, Liu T, Coelho AL, Allen RM, Carson WFt, Cavassani KA, Li X, Lukacs NW, Hogaboam CM, Dou Y, Kunkel SL. Epigenetic regulation of the alternatively activated macrophage phenotype. Blood. 2009; 114(15):3244–54. [PubMed: 19567879]
43. Solorio L, Zwolinski C, Lund AW, Farrell MJ, Stegemann JP. Gelatin microspheres crosslinked with genipin for local delivery of growth factors. J Tissue Eng Regen Med. 2010; 4(7):514–23. [PubMed: 20872738]

44. Annamalai, RT., Turner, P., Carson, W., Stegemann, J. Macrophage-mediated Degradation of Gelatin Microspheres for Release of Bone Morphogenetic Protein. Biomedocal Engineering Society Annual Meeting; Minneapolis. 2016.
45. Tiruvannamalai Annamalai R, Rioja AY, Putnam AJ, Stegemann JP. Vascular Network Formation by Human Microvascular Endothelial Cells in Modular Fibrin Microtissues. ACS Biomaterials Science & Engineering. 2016; 2(11):1914–1925.
46. Klein T, Bischoff R. Physiology and pathophysiology of matrix metalloproteases. Amino acids. 2011; 41(2):271–290. [PubMed: 20640864]
47. Anderson JM, Rodriguez A, Chang DT. Foreign body reaction to biomaterials. Seminars in Immunology. 2008; 20(2):86–100. [PubMed: 18162407]
48. Lou X, Chirila TV. Swelling Behavior and Mechanical Properties of Chemically Cross-Linked Gelatin Gels for Biomedical Use. Journal of biomaterials applications. 1999; 14(2):184–191. [PubMed: 10549004]
49. Gómez-Guillén MC, Giménez B, López-Caballero ME, Montero MP. Functional and bioactive properties of collagen and gelatin from alternative sources: A review. Food Hydrocolloids. 2011; 25(8):1813–1827.
50. Lynn AK, Yannas IV, Bonfield W. Antigenicity and immunogenicity of collagen. Journal of Biomedical Materials Research Part B: Applied Biomaterials. 2004; 71B(2):343–354.
51. Rose JB, Pacelli S, El Haj AJ, Dua HS, Hopkinson A, White LJ, Rose FRAJ. Gelatin-Based Materials in Ocular Tissue Engineering. Materials. 2014; 7(4):3106–3135. [PubMed: 28788609]
52. Turner PA, Thiele JS, Stegemann JP. Growth factor sequestration and enzyme-mediated release from genipin-crosslinked gelatin microspheres. Journal of biomaterials science Polymer edition. 2017; 28(16):1826–1846. [PubMed: 28696181]
53. Charulatha V, Rajaram A. Influence of different crosslinking treatments on the physical properties of collagen membranes. Biomaterials. 2003; 24(5):759–767. [PubMed: 12485794]
54. Thakur G, Mitra A, Rousseau D, Basak A, Sarkar S, Pal K. Crosslinking of gelatin-based drug carriers by genipin induces changes in drug kinetic profiles in vitro. Journal of Materials Science: Materials in Medicine. 2011; 22(1):115–123. [PubMed: 21107660]
55. Usta M, Piech DL, MacCrone RK, Hillig WB. Behavior and properties of neat and filled gelatins. Biomaterials. 2003; 24(1):165–172. [PubMed: 12417190]
56. Sisson K, Zhang C, Farach-Carson MC, Chase DB, Rabolt JF. Evaluation of Cross-Linking Methods for Electrospun Gelatin on Cell Growth and Viability. Biomacromolecules. 2009; 10(7): 1675–1680. [PubMed: 19456101]
57. Bigi A, Cojazzi G, Panzavolta S, Rubini K, Roveri N. Mechanical and thermal properties of gelatin films at different degrees of glutaraldehyde crosslinking. Biomaterials. 2001; 22(8):763–768. [PubMed: 11246944]
58. Tsai CC, Huang RN, Sung HW, Liang HC. In vitro evaluation of the genotoxicity of a naturally occurring crosslinking agent (genipin) for biologic tissue fixation. Journal of biomedical materials research. 2000; 52(1):58–65. [PubMed: 10906675]
59. Solorio LD, Dhami CD, Dang PN, Vieregge EL, Alsberg E. Spatiotemporal Regulation of Chondrogenic Differentiation with Controlled Delivery of Transforming Growth Factor-β1 from Gelatin Microspheres in Mesenchymal Stem Cell Aggregates. Stem cells translational medicine. 2012; 1(8):632–639. [PubMed: 23197869]
60. Patel ZS, Yamamoto M, Ueda H, Tabata Y, Mikos AG. Biodegradable gelatin microparticles as delivery systems for the controlled release of bone morphogenetic protein-2. Acta Biomaterialia. 2008; 4(5):1126–1138. [PubMed: 18474452]
61. Young S, Wong M, Tabata Y, Mikos AG. Gelatin as a delivery vehicle for the controlled release of bioactive molecules. Journal of Controlled Release. 2005; 109(1–3):256–274. [PubMed: 16266768]
62. Szabo KA, Ablin RJ, Singh G. Matrix metalloproteinases and the immune response. Clinical and Applied Immunology Reviews. 2004; 4(5):295–319.
63. Webster NL, Crowe SM. Matrix metalloproteinases, their production by monocytes and macrophages and their potential role in HIV-related diseases. Journal of Leukocyte Biology. 2006; 80(5):1052–1066. [PubMed: 16959898]

64. Shapiro SD, Campbell EJ, Kobayashi DK, Welgus HG. Immune modulation of metalloproteinase production in human macrophages. Selective pretranslational suppression of interstitial collagenase and stromelysin biosynthesis by interferon-gamma. The Journal of clinical investigation. 1990; 86(4):1204–10. [PubMed: 2170447]

65. Speidl WS, Toller WG, Kaun C, Weiss TW, Pfaffenberger S, Kastl SP, Furnkranz A, Maurer G, Huber K, Metzler H, Wojta J. Catecholamines potentiate LPS-induced expression of MMP-1 and MMP-9 in human monocytes and in the human monocytic cell line U937: possible implications for peri-operative plaque instability. FASEB journal: official publication of the Federation of American Societies for Experimental Biology. 2004; 18(3):603–5. [PubMed: 14715701]

66. Opdenakker G, Van den Steen PE, Van Damme J. Gelatinase B: a tuner and amplifier of immune functions. Trends Immunol. 2001; 22(10):571–9. [PubMed: 11574282]

67. Busiek DF, Baragi V, Nehring LC, Parks WC, Welgus HG. Matrilysin expression by human mononuclear phagocytes and its regulation by cytokines and hormones. The Journal of Immunology. 1995; 154(12):6484–6491. [PubMed: 7759883]

68. Niu Y, Li Q, Xie R, Liu S, Wang R, Xing P, Shi Y, Wang Y, Dong L, Wang C. Modulating the phenotype of host macrophages to enhance osteogenesis in MSC-laden hydrogels: Design of a glucomannan coating material. Biomaterials. 2017; 139:39–55. [PubMed: 28582717]

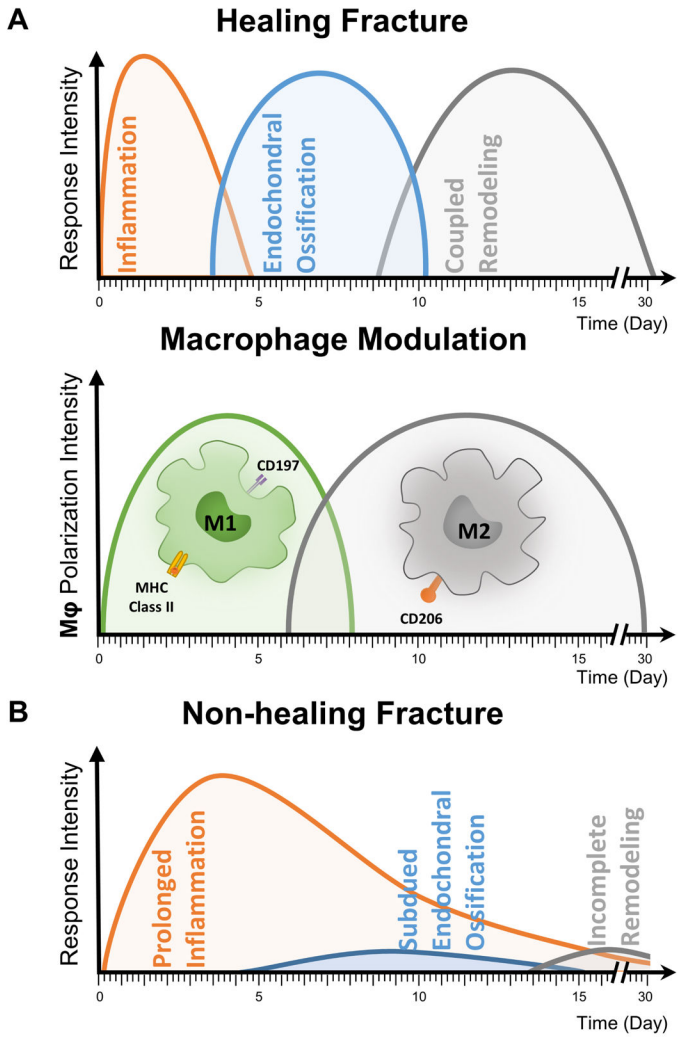

Fig. 1. Role of inflammatory cells in normal and pathological fracture healing

A) Normal fracture healing involves phases characterized by inflammation, endochondral ossification, and coupled tissue remodeling. The phenotype of local macrophages changes from pro-inflammatory (M1) to pro-reparative (M2) as bone repair proceeds. B) In non-healing fractures, the progression to the endochondral ossification is delayed or inhibited, such that new bone is not regenerated.

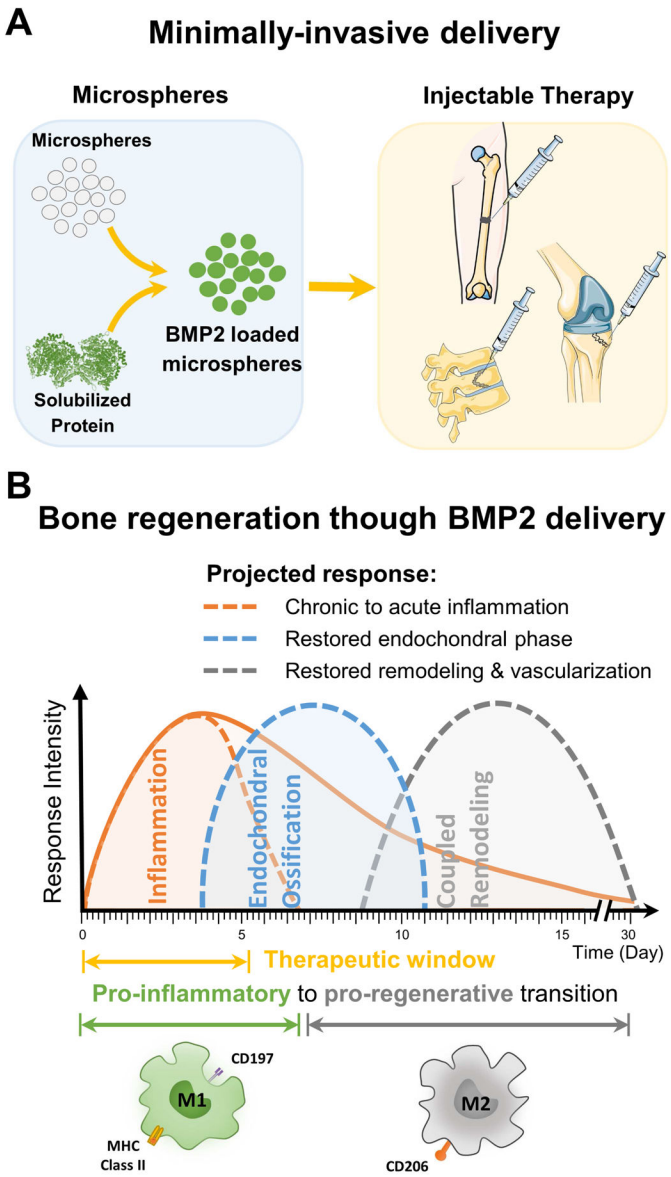

Fig. 2. Delivery of therapeutic growth factors to potentiate bone regeneration

A) Gelatin microspheres can be designed to sequester BMP2 and can be used as a minimally-invasive method of delivering growth factor to bone wounds. B) Design of microspheres to be preferentially degraded by inflammatory macrophages allows delivery of BMP2 during the late inflammation phase of healing, and promotes progression to endochondral ossification, thereby preventing delayed healing.

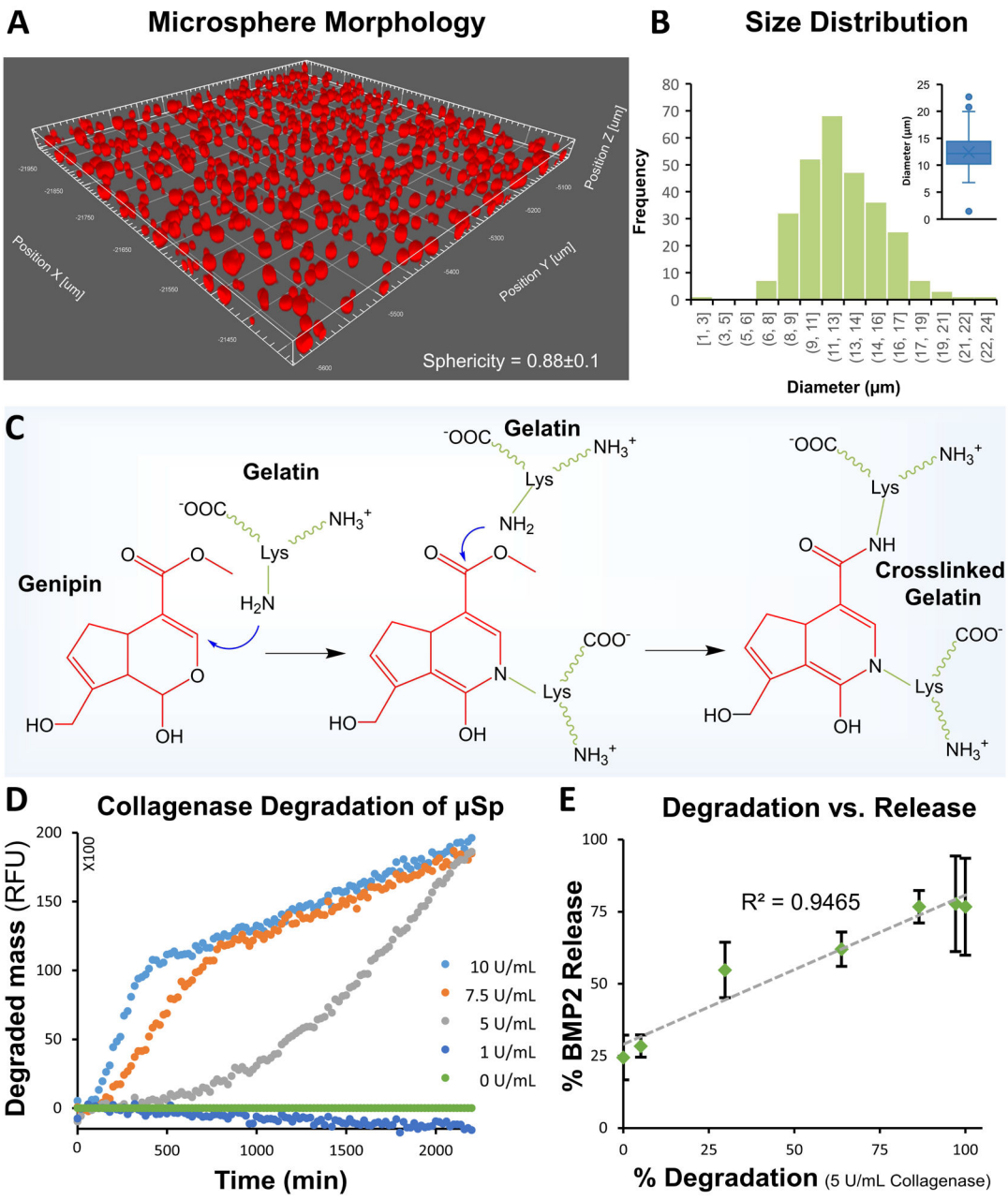

Fig. 3. Morphology, genipin crosslinking chemistry and enzymatic degradation of gelatin microspheres

A) Confocal image of microspheres show spherical morphology. B) Histogram showing the size distribution of crosslinked gelatin microspheres (inset shows the box plot of the size distribution). C) Genipin is used to crosslink lysine residues in gelatin via a two-step process. D) The degradation rate of crosslinked microspheres increased with an increase in collagenase concentration. E) Enzymatic degradation of the microspheres caused an initial burst release followed by sustained release of the remainder of the payload.

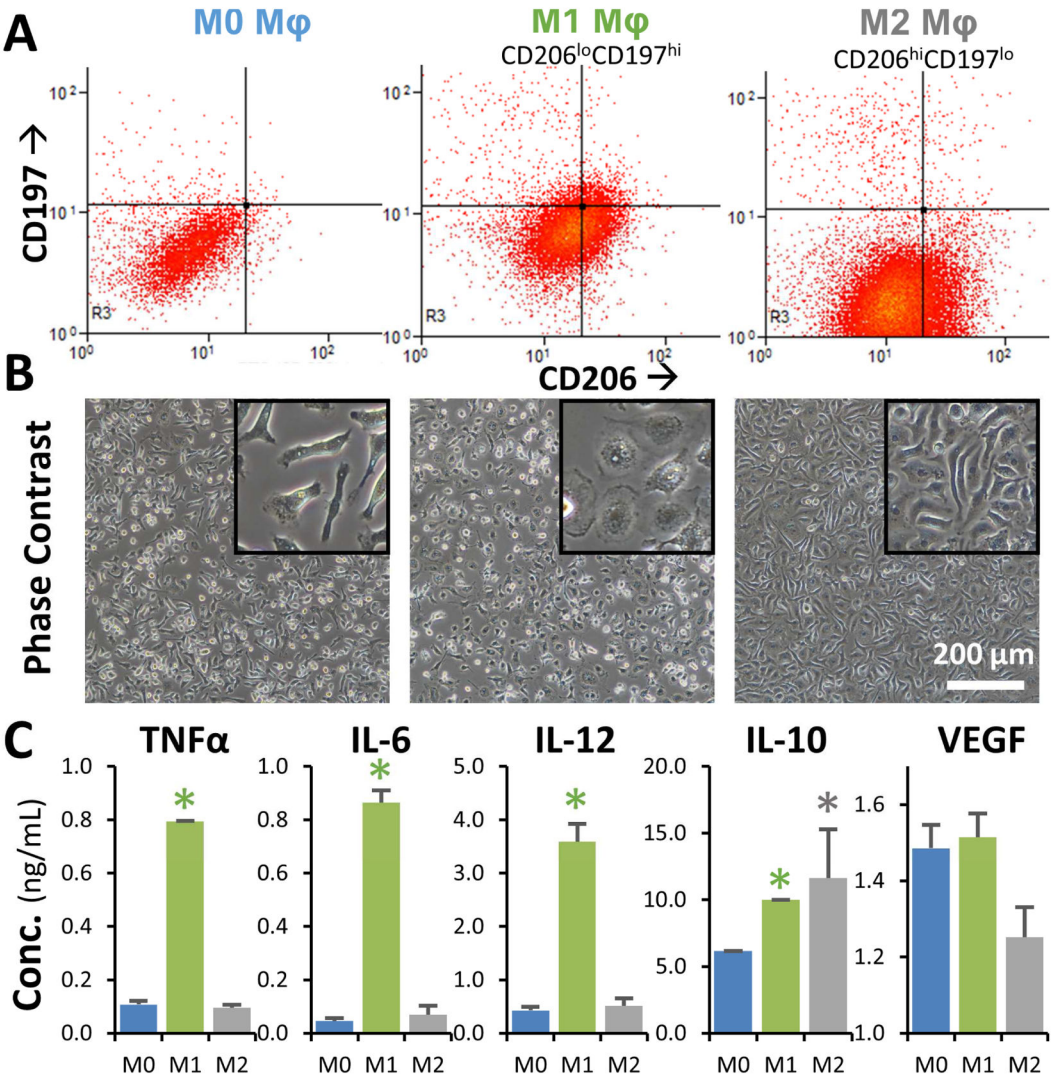

Fig. 4. Characterization of macrophage phenotype

A) Flow cytometric analysis showed that M1-treated macrophages had increased CD197 expression and reduced CD206 expression ($CD197^{hi}CD206^{lo}$), while the M2-treated population showed increased CD206 expression and reduced CD197 expression ($CD206^{hi}CD197^{lo}$). B) M1 macrophages had a 'broken-egg' morphology, while M2 macrophages exhibited a more spindle-shaped morphology (insets show magnified cell morphology). C) Cytokine secretion by M1 macrophages showed significantly higher levels of TNFα, IL-6, Il-10, relative to M2 macrophages, which had increased secretion of IL10. *$p<0.05$

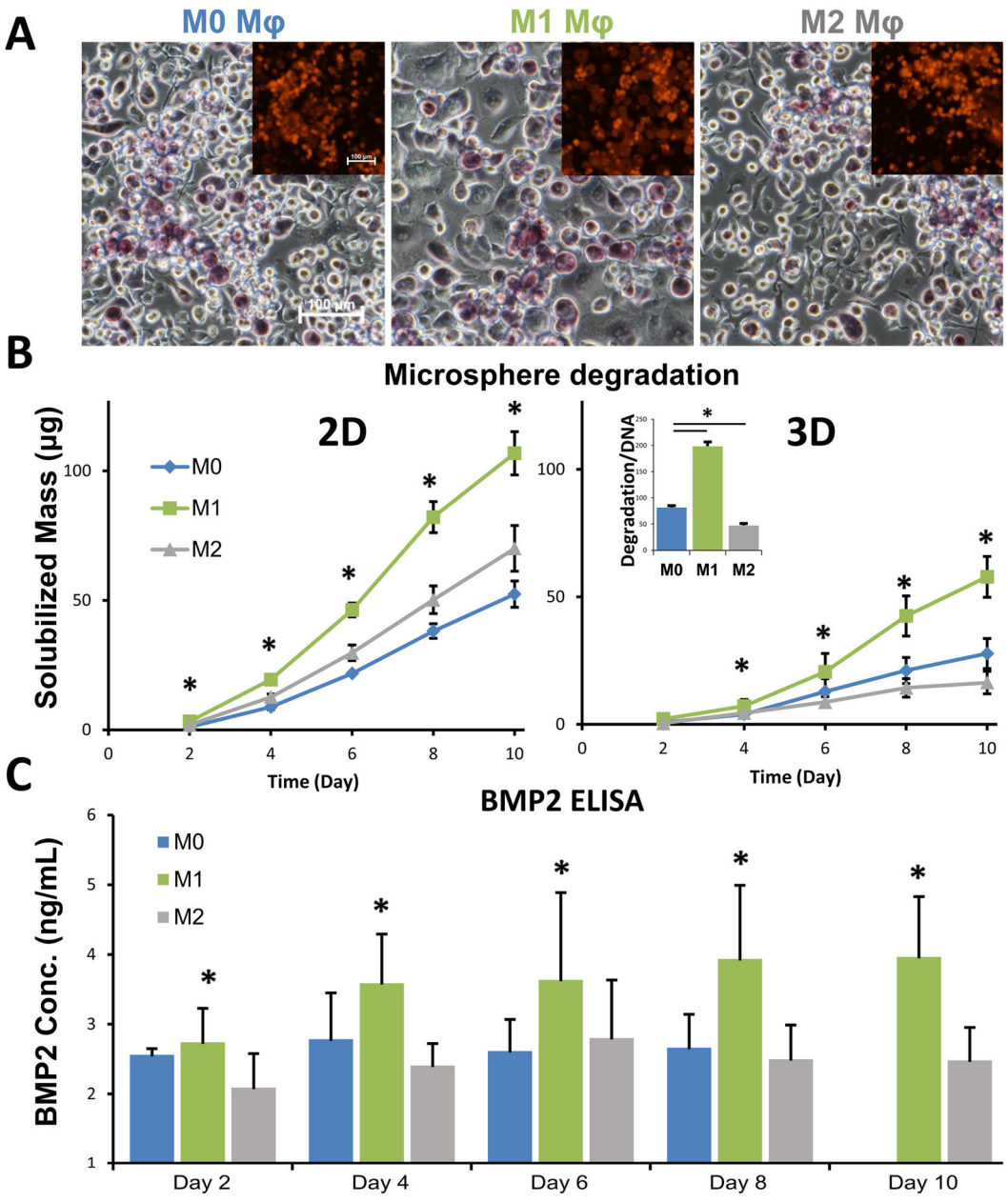

Fig. 5. Cell-mediated degradation of microspheres leads to BMP2 release

A) Macrophages degraded microspheres through enzymatic degradation (insets show fluorescent microspheres). The genipin crosslinking changed the color of the gelatin microspheres to a blue/purple color under visible light. B) At the same cell density and microsphere mass, the rate of degradation was higher when cultured in 2D wells, compared to 3D collagen matrices. The normalized degradation rate of macrophages was higher under M1 conditions compared to that of M0 and M2 (inset). C) As a result of preferential degradation, the release of BMP2 from loaded microspheres was higher from M1 macrophages compared to M0 and M2. *$p<0.05$

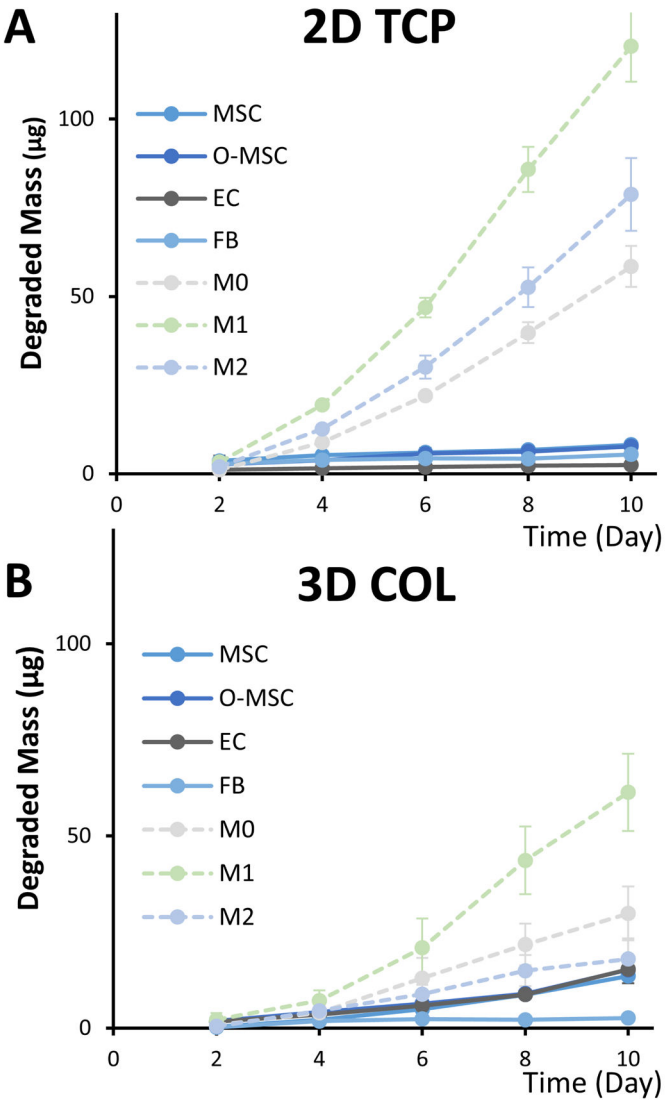

Fig. 6. Degradation rates of gelatin microspheres varied by cell type

A) In 2D cultures, macrophages of all phenotypes degraded microspheres at a faster rate than non-inflammatory cells. B) In 3D collagen gels, a similar trend was observed, though degradation by macrophages was slower in 3D than in 2D.

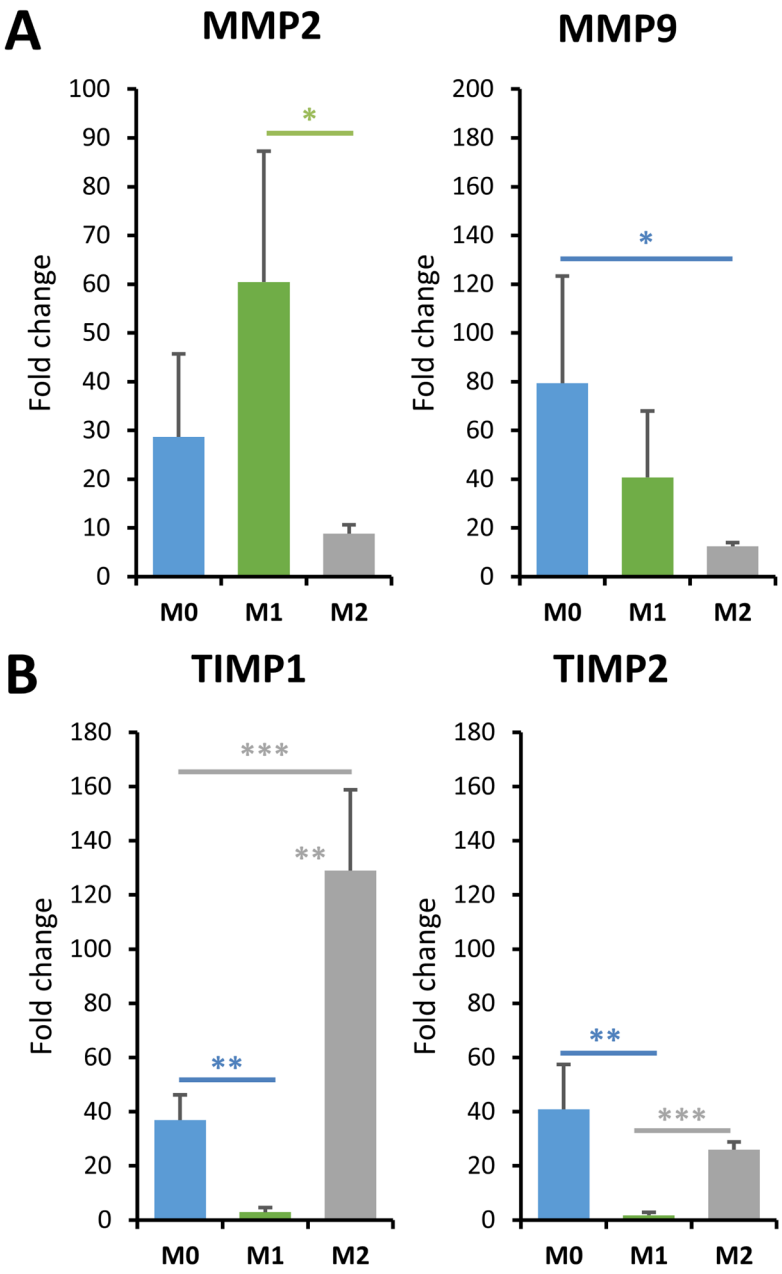

Fig. 7. Macrophage polarization affects MMP and TIMP expression

A) The skewing of macrophages to the M1 phenotype enhanced MMP2 expression, while M2 macrophages showed suppressed MMP9 expression. B) M1 macrophages showed depressed TIMP expression while skewing to the M2 phenotype enhanced TIMP1 expression. *p<0.05, **p<0.005, ***p<0.0005.

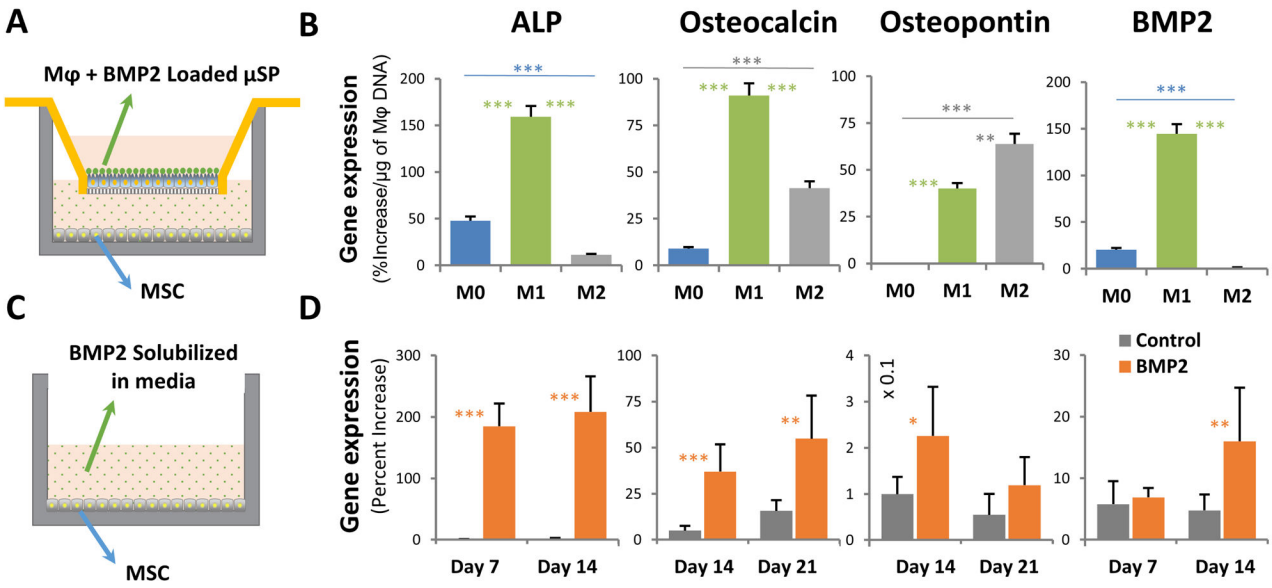

Fig. 8. BMP2 released through the degradation of microspheres stimulated MSC osteogenesis

A) A Transwell™ system was used to allow paracrine signaling between macrophage-degraded microspheres and cultured MSC. B) The BMP2 released by M1 macrophage-mediated degradation caused increased expression of osteogenic genes in MSC, compared to both M0 and M2 macrophages ($p<0.01$). C) Positive control cultures were exposed to a constant dose of 200 ng/ml of solubilized BMP2 in standard culture wells. D) Positive control cultures showed increased expression of osteogenic genes over time. *$p<0.05$, **$p<0.01$, ***$p<0.005$.

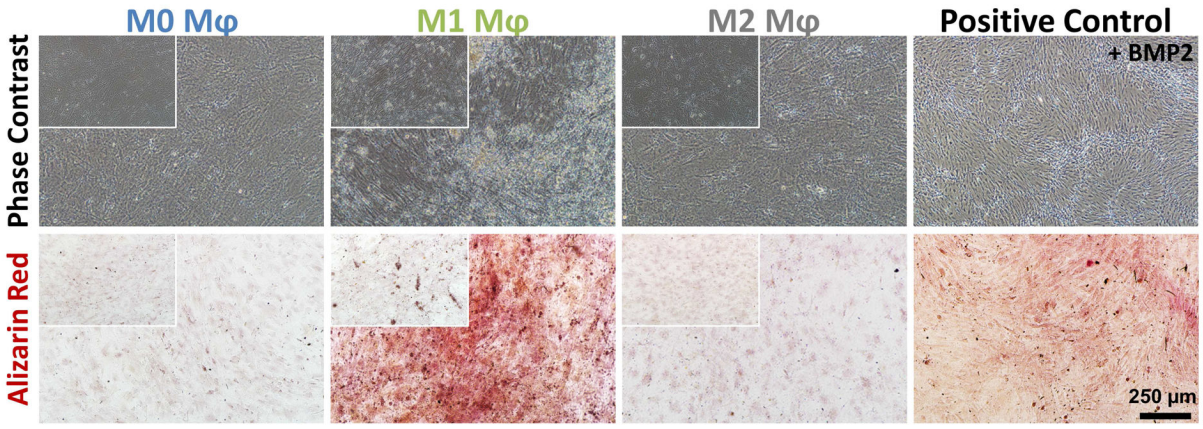

Fig. 9. BMP2 released through macrophage-mediated degradation of microspheres stimulated MSC osteogenesis and calcification

Microspheres degraded by M1 macrophages had the largest osteogenic effect, similar to positive controls containing 200 ng/mL BMP2, and markedly higher than cultures exposed to M0 and M2 macrophages. The insets show the phase contrast and alizarin red staining of the corresponding negative control wells supplied with unloaded microspheres. There is no matrix deposition/staining on the unloaded microspheres on M0, M1 or M2 conditions.